10,19

Changing the Parameters of Vacancy Formation and Self-Diffusion in a Crystal with Temperature and Pressure

© M.N. Magomedov

Institute for geothermal problems and renewable energy —
branch of the joint Institute of high temperatures of the Russian Academy of Sciences,
Makhachkala, Russia

E-mail: mahmag4@mail.ru

Received November 10, 2021
Revised November 10, 2021
Accepted November 18, 2021

An analytical method for calculating the parameters of the electroneutral vacancies formation and self-diffusion of atoms in a single-component crystal is proposed. The method is based on the 4-parameters pairwise Mie–Lennard-Jones interatomic interaction potential. The method allows calculating all the activation processes parameters: Gibbs energy, enthalpy, entropy and volume for both the vacancy formation process and the self-diffusion process. The method is applicable at any pressure (P) and temperature (T). The temperature dependencies of the activation processes parameters for gold are calculated from $T = 10\,\mathrm{K}$ to $1330\,\mathrm{K}$ along two isobars $P = 0$ and $24\,\mathrm{GPa}$. It is shown that at low temperatures, due to quantum regularities, activation parameters strongly depend on temperature, and the entropy of activation processes in this region has a negative value. In the high temperature region, the probability of vacancy formation and the self-diffusion coefficient pass into classical Arrhenius dependencies with a weakly temperature-dependent enthalpy and with a positive value of the activation process entropy. Good agreements were obtained with the estimates of activation parameters for gold known from the literature. The values of activation parameters at $T = 0\,\mathrm{K}$ were discussed.

Keywords: vacancy, self-diffusion, interatomic potential, gold, state equation, thermal expansion.

DOI: 10.21883/PSS.2022.04.53504.240

1. Introduction

Studies of activation processes (i.e. formation of electroneutral vacancies and self-diffusion) in a crystal of a single-component substance are carried out for long, and the results of these works are outlined in reviews [1–6]. The enthalpies of vacancy formation (h_v) and self-diffusion (h_d) were measured by different methods, which made it possible to objectively estimate these energy parameters of activation processes.

But these processes were studied experimentally only in the region of high temperatures ($T \gg \Theta$) and low pressures ($P = 1\,\mathrm{atm}$), where these activation processes exert the maximum impact on crystal properties and, therefore, the magnitude of activation parameters can be estimated experimentally. Here Θ is Debye temperature. Along with that, while enthalpy of vacancy formation and self-diffusion (h_i) can be reliably measured in the region of high temperatures, activation process volume (v_i) is estimated very approximately even at $T \gg \Theta$ [7]. There are yet no experimental methods for estimation of entropy (s_i) of activation processes [8,9] ($i = \mathrm{v}, \mathrm{d}$).

As regards the theoretical study of activation process parameters, many models were suggested both for the formation of electroneutral vacancies and for self-diffusion in a crystal [8–10]. However, none of the suggested calculation procedures (neither the analytical not the computer one) made it possible to describe both the isobaric temperature dependence and the isothermal baric dependence of all activation parameters in a crystal of a single-component substance.

Meanwhile, many fundamental questions have still not been clearly answered:

How does a transition from high-temperature diffusion (described by the Arrhenius formula) to quantum diffusion occur at low temperatures, where the Arrhenius equation does not work?

What is the isobaric (at $P = 1\,\mathrm{atm}$) temperature dependence of functions $s_i(T)$ and $v_i(T)$, starting from $T = 0\,\mathrm{K}$ and up to the crystal melting temperature?

How do these isobaric dependences of functions $s_i(T)$ and $v_i(T)$ change at a pressure increase on the isobar?

In this respect, this paper suggests an analytical method for studying the thermal and baric dependences of activation processes in a crystal of a single-component substance. By the example of a gold crystal, this method was used for the first time to calculate the temperature dependences of all activation parameters, starting from $T = 10\,\mathrm{K}$ and up to the melting temperature. Thereat, all the calculations were performed along two isobars: at $P = 0\,\mathrm{GPa} \cong 1\,\mathrm{atm}$ (where the experimental estimates were obtained) and at $P = 24\,\mathrm{GPa}$.

2. Method for calculation of vacancy formation probability

Let us represent a single crystal of a single-component substance from N atoms as a structure of $N + N_v$ cells having the same size, where N_v cells are vacant and uniformly distributed across crystal volume V. We will assume that atoms in the system can be in two states: localized (L-) and delocalized (D-). The atom in the L-state is localized in a cell formed by the nearest neighbors and has only the oscillatory degrees of freedom. The atom in the D-state has access to the whole system volume and has only the translational degrees of freedom. Atoms in the L- and D-state will be called L- and D-atoms for brevity.

The system volume is equal to the sum of volumes v_a, falling on one (occupied or vacant) atomic cell the shape of which is considered to be spherical

$$V = \frac{\pi}{6k_p}(N + N_v) \cdot c^3 = \frac{v_a}{k_p} \frac{N}{(1 - \phi_v)}, \quad (1)$$

$$v_a = \frac{\pi}{6} \cdot c^3 = \frac{V}{N} \cdot k_p \cdot (1 - \phi_v),$$

$$c_o = \left(\frac{6k_pV}{\pi N}\right)^{1/3} = \left[\frac{6v_a(\phi_v = 0)}{\pi}\right]^{1/3}. \quad (2)$$

Here $\phi_v = N_v/(N + N_v)$ — probability of finding a vacant cell in the system, $c = c_o(1 - \phi_v)^{1/3}$ — distance between centers of the nearest cells, k_p — packing coefficient for a structure of $N + N_v$ spherical cells, c_o — distance between centers of the nearest cells in the initial (not relaxed into the vacancy-activated state) vacansion-free (at $N_v = 0$) virtual lattice (this is indicated by index „o“).

The following expression can be used when there are no different gradients for the probability of atom detection in a ball layer with thickness dr at distance r from the cell center

$$\phi_c(r)dr = C_c \cdot \exp\left(-\frac{r^2}{2\langle r^2\rangle}\right) dr,$$

where C_c — normalization constant, $\langle r^2\rangle$ — root-mean-square deviation of the atom from the cell center.

Let us divide the ball layer into k_n^o sections, where k_n^o is the number of all cells (both occupied and vacant) nearest to the given atom. Representing the atom as a cluster of probability density and considering quantity $\phi_c(r)dr$ as the probability of simultaneous atomic displacement in all $k_n^o/2$ radial directions, the following can be adopted for the probability of atomic displacement in one j-th direction

$$\phi_j(r)dr = \frac{2}{(\pi k_n^o\langle r^2\rangle_j)^{1/2}} \cdot \exp\left(-\frac{r^2}{2\langle r^2\rangle_j}\right) dr.$$

We will assume that an atom can leave a cell if the amplitude of its oscillation in a cell exceeds $c_{jo}/2$, where c_{jo} is distance between the centers of the nearest cells in j-th direction in an initial vacansion-free virtual lattice (therefore the index „o“). Then we can determine the vacancy formation probability as the arithmetic mean from the probabilities of escape from a cell in any of $k_n^o/2$ directions. For an isotropic model, this gives the following expression [11,12]:

$$\phi_v(\rho, T) = \frac{N_v(\rho, T)}{N + N_v} = \frac{2}{\pi^{1/2}} \int\limits_{c_o/[2(k_n^o\langle r^2\rangle)^{1/2}]}^{\infty} \exp(-t^2)dt$$

$$= 1 - \mathrm{erf}\left(\frac{c}{2(k_n^o\langle r^2\rangle)^{1/2}}\right), \quad (3)$$

where $\rho = N/V$ is density of atom quantity; the probability integral has the form [13]:

$$\mathrm{erf}(x) = \frac{2}{\pi^{1/2}} \int\limits_0^x \exp(-t^2)dt. \quad (4)$$

While determining function $\langle r^2\rangle$ for a system of L- and D-atoms, their different motion pattern must be taken into account. Since L-atoms have only oscillatory degrees of freedom, while D-atoms have (by definition) only translational degrees of freedom, we will present the function $\langle r^2\rangle$ as

$$\langle r^2\rangle = (1 - x_d)\langle r^2\rangle_L + x_d\langle r^2\rangle_D. \quad (5)$$

Here $\langle r^2\rangle_L$ and $\langle r^2\rangle_D$ — root mean square atomic displacement in the L- and D-state, respectively, x_d — share of atoms in the D-state.

Defining the function $\langle r^2\rangle_L$ using the harmonic oscillator model [14] and considering that all L-atoms oscillate with the same frequency (the Einstein model), we obtain

$$\langle r^2\rangle_L = \frac{\hbar^2 k_B T}{m(k_B\Theta_{Eo})^2 f_y(\Theta_{Eo}/T)}, \quad (6)$$

where $\hbar$ — the Planck constant, k_B — the Boltzmann constant, m — atomic mass, Θ_{Eo} — Einstein temperature in a vacansion-free lattice (therefore the index „o“), function $f_y(y_w)$ arises due to accounting of quantum effects and has the form

$$f_y(y_w) = \frac{2}{y_w} \cdot \frac{[1 - \exp(-y_w)]}{[1 + \exp(-y_w)]}, \quad y_w = \frac{\Theta_{Eo}}{T}. \quad (7)$$

In order to determine quantity $\langle r^2\rangle_D$, we must know the size of the accessible region for motion of a D-atom in the lattice within the time equal to the L-atom oscillation period. Since the system is homogeneous and its whole volume is accessible for a D-atom, the configuration integral for a D-atom in the lattice of equal-sized $N + N_v$ cells can be presented as

$$In = \frac{1}{V} \int\limits_V \exp\left(-\frac{U}{k_BT}\right) dV$$

$$= \frac{N + N_v}{V} \int\limits_{V/(N+N_v)} \exp\left(-\frac{U}{k_BT}\right) 4\pi r^2 dr,$$

where U is the potential energy of interaction of the considered D-atom with its environment.

Proceeding to variable $t = r/c_o$, we obtain the following taking into account (2)

$$In = 24k_p \cdot \int_0^{\alpha_3} \exp\left(-\frac{U}{k_B T}\right) t^2 dt,$$

Here the upper limit of integration α_3 defines the radius (in relative units) of the region for motion of a D-atom in a lattice of $N + N_v$ identical spherical cells. We will find it from the boundary condition which must be met by function In:

$$\lim_{U/(k_B T)=0} In = 1.$$

The following value is obtained: $\alpha_3 = 0.5/k_p^{1/3}$. Therefore, the diameter of the accessibility region for a D-atom in the lattice structure within the L-atom oscillation period will be equal to

$$\lambda_3 = 2c_o\alpha_3 = c_o/k_p^{1/3}. \quad (8)$$

On the other hand, an atom goes over from the L- to the D-state when its velocity ensures its covering (within a half-period of oscillation in the L-state ($\tau/2$)) a distance equal to the accessibility region radius for a D-atom in the initial vacansion-free (not relaxed into the activated state) lattice structure: $\lambda_3/2$. Thus, atom velocity at a transition from the L- to the D-state must exceed $v_{min} = (\lambda_3/2)/(\tau/2)$. Since only a third part of displacements take place in the chosen direction due to model isotropy, the following can be adopted for root mean square displacement of a D-atom as the time of a full oscillation period of a L-atom

$$\langle r^2\rangle_D = \frac{(v_{min}\tau)^2}{3} = \frac{1}{3}\left(\frac{c_o}{k_p^{1/3}}\right)^2. \quad (9)$$

Formulas (3)–(9) give an expression for the vacancy formation probability in the form [11,12]:

$$\phi_v = 1 - \mathrm{erf}\left(\frac{c_o}{2(k_p^o\langle r^2\rangle)^{1/2}}\right) = 1 - \mathrm{erf}\left[\left(\frac{E_v}{k_B T}\right)^{1/2}\right] = \mathrm{erfc}\left[\left(\frac{E_v}{k_B T}\right)^{1/2}\right]. \quad (10)$$

Here E_v is energy of vacant cell creation in a vacansion-free lattice, defined by the expression

$$E_v = \frac{E_L}{1 + x_d[(C_D E_L/k_B T) - 1]}, \quad (11)$$

where the following is introduced

$$E_L = \frac{c_o^2 k_B T}{4k_n^o\langle r^2\rangle_L} = \frac{m}{k_n^o}\left(\frac{c_o^2 k_B \Theta_{Eo}}{2\hbar}\right)^2 f_y\left(\frac{\Theta_{Eo}}{T}\right), \quad (12)$$

$$C_D = \frac{4k_n^o}{3k_p^{2/3}}. \quad (13)$$

If $T > \Theta_{Eo}$, the function E_L does not depend on temperature, and $E_v > k_B T$ is true up to the melting temperature. Then expression (10) can be with good accuracy substituted by an exponential Arrhenius dependence [13]:

$$\phi_v = 1 - \mathrm{erf}\left[\left(\frac{E_v}{k_B T}\right)^{1/2}\right] \cong \left(\frac{k_B T}{\pi E_v}\right)^{1/2} \exp\left(-\frac{E_v}{k_B T}\right). \quad (14)$$

However, when $T < \Theta_{Eo}$, the functions E_L and E_v have a linear temperature dependence, which violates the Arrhenius temperature dependence for the vacancy formation probability. It can be easily seen from (14) that the inequality is fulfilled

$$\phi_v(\rho, T = 0\,\mathrm{K}) > 0.$$

3. Determining the probability of atom delocalization in a crystal

We determine the share of D-atoms using the Maxwell distribution for atom kinetic energy, which is true not only for gas, but also for the liquid, amorphous and crystalline phases [15,16]. The share of D-atoms is determined as the share of atoms having a kinetic energy above the threshold value E_d — atom delocalization energy

$$x_d(\rho, T) = \frac{N_d(\rho, T)}{N} = \frac{2}{\pi^{1/2}} \int_{E_d/(k_B T)}^{\infty} t^{1/2}\exp(-t)dt = 2\left(\frac{E_d}{\pi k_B T}\right)^{1/2} \cdot \exp\left(-\frac{E_d}{k_B T}\right) + 1 - \mathrm{erf}\left[\left(\frac{E_d}{k_B T}\right)^{1/2}\right], \quad (15)$$

where E_d is the required energy for atom transition from the L- to the D-state.

For atom transition from the L-state to the D-state, its velocity must be not less than $v_{min} = \lambda_3/\tau$, where τ is the oscillation period of a L-atom in a cell. Starting with this velocity, an atom may leave a cell. Since the period of atom oscillation in a cell for the Einstein crystal model is equal to [14]:

$$\tau = \frac{2\pi\hbar}{k_B\Theta_{Eo}} = \frac{8\pi\hbar}{3k_B\Theta_o}, \quad (16)$$

the function E_d can be defined as [17]:

$$E_d = \frac{3}{2} m v_{min}^2 \cdot f_y(y_w) = \left(\frac{3}{8\pi^2}\right) m\left(\frac{c_o k_B \Theta_{Eo}}{\hbar k_p^{1/3}}\right)^2 f_y(y_w) = C_{LD}E_L = E_{d1} f_y(y_w). \quad (17)$$

Here the following is introduced

$$E_{\mathrm{d1}} = E_{\mathrm{d}}\big(f_y(y_w) = 1\big) = \frac{3m}{8k_{\mathrm{p}}^{2/3}}\left(\frac{3c_{\mathrm{o}}k_{\mathrm{B}}\Theta_{\mathrm{o}}}{4\pi\hbar}\right)^2,$$

$$C_{\mathrm{LD}} = \frac{3k_n^{\mathrm{o}}}{2\pi^2k_{\mathrm{p}}^{2/3}} = \left(\frac{9}{8\pi^2}\right)C_{\mathrm{D}}, \qquad (18)$$

here Θ is the Debye temperature, related to the Einstein temperature by a relation: $\Theta = (4/3)\Theta_{\mathrm{E}}$ [18, Chap. 13; 19, Chap. 2].

Inequality $E_{\mathrm{d}} > E_{\mathrm{v}} > k_{\mathrm{B}}T_{\mathrm{m}}$ is true for most substances (except quantum crystals) up to the melting temperature (T_{m}). Therefore, the incomplete gamma-function in (15) in the whole temperature range from $T = 0\,\mathrm{K}$ to T_{m} can be approximated by an Arrhenius formula [13]:

$$x_{\mathrm{d}}(\rho, T) = 2\left(\frac{E_{\mathrm{d}}}{\pi k_{\mathrm{B}}T}\right)^{1/2}\exp\left(-\frac{E_{\mathrm{d}}}{k_{\mathrm{B}}T}\right)\left[1 + \frac{k_{\mathrm{B}}T}{2E_{\mathrm{d}}} - \left(\frac{k_{\mathrm{B}}T}{2E_{\mathrm{d}}}\right)^2 + \ldots\right] \cong 2\left(\frac{E_{\mathrm{d}}}{\pi k_{\mathrm{B}}T}\right)^{1/2}\exp\left(-\frac{E_{\mathrm{d}}}{k_{\mathrm{B}}T}\right). \qquad (19)$$

The function E_{d} in (19), like E_{v} in (14), at $T < \Theta_{\mathrm{Eo}}$ has a linear temperature dependence, which violates the Arrhenius temperature dependence for the atom delocalization probability. Thereat, an inequality follows from (14): $x_{\mathrm{d}}(\rho, T = 0\,\mathrm{K}) > 0$.

Our papers [11,12,17,20–22] showed that the above-mentioned formalism from (10)–(19) makes it possible to study the activation parameters from $T = 0\,\mathrm{K}$ and up to a transition to the liquid phase. It can be easily seen that the formalism from (10)–(19) makes it possible to study the change in functions $\phi_{\mathrm{v}}(\rho, T)$ and $x_{\mathrm{d}}(\rho, T)$ both in case of an isochoric temperature change and in case of an isothermal change of crystal density.

4. Thermodynamic parameters of activation processes

Thermodynamic determination of activation (vacancy formation and self-diffusion) parameters, based on the formulas of equilibrium and reversible thermodynamics [1–6,19], is as follows

$$g_i = -k_{\mathrm{B}}T\ln(A_i),$$

$$h_i = -\left(\frac{\partial\ln(A_i)}{\partial[1/(k_{\mathrm{B}}T)]}\right)_P = g_i + Ts_i,$$

$$s_i = -\left(\frac{\partial g_i}{\partial T}\right)_P = -\left(\frac{\partial g_i}{\partial T}\right)_V - \alpha_P V\left(\frac{\partial g_i}{\partial V}\right)_T = \frac{h_i - g_i}{T},$$

$$v_i = -\left(\frac{\partial g_i}{\partial P}\right)_T = -\frac{V}{B_T}\left(\frac{\partial g_i}{\partial V}\right)_T. \qquad (20)$$

Here g_i, h_i, s_i, v_i are Gibbs energy, enthalpy, entropy and volume of an activation process (index $i = \mathrm{v}$ or d for vacancy formation ($A_i = \phi_{\mathrm{v}}$) or for self-diffusion ($A_i = x_{\mathrm{d}}$)), respectively. Function $\alpha_P = (1/V)(\partial V/\partial T)_P$ is isobaric coefficient of thermal expansion, $B_T = -V(\partial P/\partial V)_T$ is isothermal elastic modulus.

Supposing that the characteristic temperature does not change under isochoric heating (i.e. under condition $(\partial\Theta_{\mathrm{o}}/\partial T)_V = 0$), and assuming approximations (14) and (19), we can obtain from (10)–(19) the expressions for Gibbs energy, enthalpy, entropy and volume of the activation process in the form [11,12,17]:

for the vacancy formation process

$$g_{\mathrm{v}} = -k_{\mathrm{B}}T\cdot\ln(\phi_{\mathrm{v}}) = E_{\mathrm{v}}\left[1 + \left(\frac{k_{\mathrm{B}}T}{2E_{\mathrm{v}}}\right)\ln\left(\frac{\pi E_{\mathrm{v}}}{k_{\mathrm{B}}T}\right)\right],$$

$$h_{\mathrm{v}} = k_{\mathrm{B}}T\phi_{\mathrm{E}}\left\{1 - t_y + \alpha_P T\left[(2 - t_y)\gamma_{\mathrm{o}} - \frac{2}{3}\right]\right\},$$

$$\frac{s_{\mathrm{v}}}{k_{\mathrm{B}}} = \frac{h_{\mathrm{v}} - g_{\mathrm{v}}}{k_{\mathrm{B}}T},$$

$$\frac{v_{\mathrm{v}}}{v_0} = \frac{k_{\mathrm{B}}T}{B_T v_0}\phi_{\mathrm{E}}\left[(2 - t_y)\gamma_{\mathrm{o}} - \frac{2}{3}\right], \qquad (21)$$

for the self-diffusion process

$$g_d = -k_{\mathrm{B}}T\cdot\ln(x_{\mathrm{d}}) = E_{\mathrm{d}}\left[1 - \left(\frac{k_{\mathrm{B}}T}{2E_{\mathrm{d}}}\right)\ln\left(\frac{4E_{\mathrm{d}}}{\pi k_{\mathrm{B}}T}\right)\right],$$

$$h_{\mathrm{d}} = E_{\mathrm{d}}\left\{1 - t_y + \alpha_P T\left[(2 - t_y)\gamma_{\mathrm{o}} - \frac{2}{3}\right]\right\},$$

$$\frac{s_{\mathrm{d}}}{k_{\mathrm{B}}} = \frac{h_{\mathrm{d}} - g_{\mathrm{d}}}{k_{\mathrm{B}}T} = \frac{E_{\mathrm{d}}}{k_{\mathrm{B}}T}\left\{\left(\frac{k_{\mathrm{B}}T}{2E_{\mathrm{d}}}\right)\ln\left(\frac{4E_{\mathrm{d}}}{\pi k_{\mathrm{B}}T}\right) - t_y + \alpha_P T\left[(2 - t_y)\gamma_{\mathrm{o}} - \frac{2}{3}\right]\right\},$$

$$\frac{v_{\mathrm{d}}}{v_0} = \frac{E_{\mathrm{d}}}{B_T v_0}\left[(2 - t_y)\gamma_{\mathrm{o}} - \frac{2}{3}\right]. \qquad (22)$$

Here $\gamma_{\mathrm{o}} = -[\partial\ln(\Theta_{\mathrm{Eo}})/\partial\ln(V)]_T$ — the first Grüneisen parameter for a vacansion-free crystal, v_0 — volume per atom at $P = 0$ and $T = 0\,\mathrm{K}$,

$$t_y(y_w) = -\frac{\partial\ln(f_y)}{\partial\ln(y_w)} = 1 - \frac{2y_w\exp(y_w)}{[\exp(2y_w) - 1]},$$

$$\phi_{\mathrm{E}} = \left(\frac{E_{\mathrm{v}}}{k_{\mathrm{B}}T}\right)\left[1 + x_{\mathrm{d}}C_{\mathrm{D}}\left(\frac{E_{\mathrm{v}}}{k_{\mathrm{B}}T}\right)\frac{E_{\mathrm{d}}}{k_{\mathrm{B}}T}G_{\mathrm{d}}\right],$$

$$G_{\mathrm{d}} = 1 - \frac{k_{\mathrm{B}}T}{C_{\mathrm{D}}E_{\mathrm{L}}} - \frac{k_{\mathrm{B}}T}{E_{\mathrm{d}}}. \qquad (23)$$

Expressions (11), (21)–(23) show that the consideration of D-atoms (i.e. function x_{d}) reduces quantities E_{v} and g_{v} and increases the values of h_{v}, s_{v} and v_{v}/v_0. This is due to the fact that the necessary energy for isobaric generation of a vacancy is greater if the formation of D-atoms is considered, because a part of energy is consumed in atom delocalization. This fact was not taken into account in any of the current analytical theories, and these theories were unable to correctly estimate the vacansion parameters in the melting region where the share and role of D-atoms become considerable [21,22].

5. Method for calculating the self-diffusion coefficient of a crystal

Diffusion coefficient D_f is equal to the number of atoms carried over through a unit area, perpendicular to the chosen direction, in unit time, at a unity concentration gradient in the given direction. Thus, the number of atoms carried over through area S_{kr} within time t at concentration gradient $\text{grad}(Conc)$, is equal to

$$M_{\text{tr}} = -D_f S_{\text{kr}} t \,\text{grad}(Conc). \tag{24}$$

This is the first Fick's Law for a stationary flow [2–4,19]. The minus sign indicates that the substance flow vector is opposite to the vector of concentration scalar field gradient.

For simplicity, let us consider the case of „flat self-diffusion" in the bulk of a single-component crystal, i.e. when the atom flow is in one direction perpendicular to the cross-section plane. Then the following expression can be adopted for the gradient of vacancy concentration at the distance of the accessibility region for a D-atom: $\lambda_3 = c_{\text{o}}/k_{\text{p}}^{1/3}$:

$$-\text{grad}(Conc) = \frac{1}{\lambda_3}\left[\left(\frac{1}{\lambda_3}\right)^3 - \phi_{\text{v}}\left(\frac{1}{\lambda_3}\right)^3\right] = \frac{1-\phi_{\text{v}}}{\lambda_3^4} = \frac{(1-\phi_{\text{v}})k_{\text{p}}^{4/3}}{c_{\text{o}}^4}. \tag{25}$$

Thus, expression (24) is reduced to

$$M_{\text{tr}} = S_{\text{kr}} k_{\text{p}}^{4/3} D_f \cdot \frac{\tau(1-\phi_{\text{v}})}{2c_{\text{o}}^4}. \tag{26}$$

For the Einstein crystal model, the atom oscillation period in a vacansion-free (because λ_3 is determined for this system) lattice is determined by formula (16). The crystal cross-section area is equal to $S_{\text{kr}} = N_{\text{cell}}\, s_{\text{cell}}/k_{\text{p}}^{2/3}$, where N_{cell} is number of cells (both occupied by atoms and vacant), being in the cross-section plane; coefficient $k_{\text{p}}^{2/3}$ takes into account the density of spherical atom packing in the cross-section plane; s_{cell} is average area of one cell (both occupied by an atom and vacant), which, according to (1), is determined as follows:

$$s_{\text{cell}} = \pi\left(\frac{c}{2}\right)^2 = \frac{\pi}{4}\left[c_{\text{o}}(1-\phi_{\text{v}})^{1/3}\right]^2 \cong \frac{\pi}{4}c_{\text{o}}^2.$$

Therefore, we obtain from (11)–(16) the following number of atoms [12,17] carried over through area S_{kr} within time $t = \tau/2$ and with vacancy concentration gradient (25):

$$M_{\text{tr}} = N_{\text{cell}}\frac{\pi c^2}{4} D_f \cdot \frac{4\pi\hbar k_{\text{p}}^{2/3}(1-\phi_{\text{v}})}{3k_{\text{B}}\Theta_{\text{o}}c_{\text{o}}^4} \cong N_{\text{cell}} D_f \cdot \frac{\pi^2\hbar k_{\text{p}}^{2/3}}{3k_{\text{B}}\Theta_{\text{o}}c_{\text{o}}^2}(1-\phi_{\text{v}}). \tag{27}$$

On the other hand, only $N_{\text{cell}}\,(1-\phi_{\text{v}})$ from N_{cell} cells in the cross-section plane are occupied by atoms. Only $N_{\text{cell}}(1-\phi_{\text{v}})x_{\text{d}}$ from them are in the D-state. Only 1/6 from the specified $N_{\text{cell}}(1-\phi_{\text{v}})x_{\text{d}}$ atoms will be carried over perpendicularly to the considered area along the considered direction. It should be noted that multiplier 1/6 is true only for equilibrium self-diffusion, because, if a motive force is present, one of the six directions will have a higher priority over the other directions. Thus, the following substance amount will be carried over through the chosen area within time $\tau/2$ [12,17]:

$$M_{\text{tr}} = x_{\text{d}} \cdot N_{\text{cell}} \cdot f_{\text{cor}} \cdot \frac{(1-\phi_{\text{v}})}{6}. \tag{28}$$

Here f_{cor} is „correlation factor", arising due to consideration of a nonzero probability that an atom, which escaped to a vacancy, can return at once without contributing to the diffusion [2,3,12].

Comparison of (27) and (28) yields an expression for the coefficient of self-diffusion in the bulk of a single-component crystal

$$D_f(\rho,T) = D_{\text{d}}(\rho)\cdot x_{\text{d}}(\rho,T) = D_{\text{d}}(\rho)\cdot\exp\left[-\frac{g_{\text{d}}(\rho,T)}{k_{\text{B}}T}\right] = D_{\text{d}}(\rho)\cdot\exp\left[\frac{s_{\text{d}}(\rho,T)}{k_{\text{B}}}\right]\cdot\exp\left[-\frac{h_{\text{d}}(\rho,T)}{k_{\text{B}}T}\right]. \tag{29}$$

The following pre-exponential multiplier is introduced here:

$$D_{\text{d}}(\rho) = f_{\text{cor}}\cdot\frac{k_{\text{B}}\Theta_{\text{o}}c_{\text{o}}^2}{2\pi^2\hbar k_{\text{p}}^{2/3}}. \tag{30}$$

The physical sense of multiplier $D_{\text{d}}(\rho)$ is that this is a self-diffusion coefficient which can theoretically be in case of isochoric ($\rho = N/V = \text{const}$) delocalization of all crystal atoms (i.e. at $x_{\text{d}}(\rho, T\to\infty) = 1$):

$$D_{\text{d}}(\rho) = \lim_{\substack{T\to\infty,\\ \rho=\text{const}}}\frac{D_f(\rho,T)}{x_{\text{d}}(\rho,T)} = \lim_{\substack{T\to\infty,\\ \rho=\text{const}}} D_f(\rho,T). \tag{31}$$

It should be noted that dependence of the self-diffusion coefficient on $P-T$-arguments in experiments is usually described by an exponential Arrhenius dependence, which is as follows [2,3,5]:

$$D_f(P,T) = D_{\text{o}}(P)\exp\left[-\frac{h_{\text{d}}(P)}{k_{\text{B}}T}\right]. \tag{32}$$

It is assumed that quantities D_{o} and h_{d} do not depend on temperature.

Expressions (15)–(19) and (29), (30) make it possible to calculate the dependence of the self-diffusion coefficient on density and temperature $D_f(\rho,T)$ for a crystal of a monoatomic substance, based on its structure (k_n^{o}), atomic mass m and Debye temperature Θ. It has been shown that this method describes the function $D_f(\rho,T)$ well, both at melting temperatures [12,17] and at $T = 0\,\text{K}$ [12,23].

6. Calculations of the state equation and properties of a gold crystal

Formulas (10)–(23) and (29), (30) include the following functions: Θ_o — Debye temperature for a vacansion-free crystal, $\gamma_o = -[\partial \ln(\Theta_o)/\partial \ln(V)]_T$ — the first Grüneisen parameter, $\alpha_P = (1/V)(\partial V/\partial T)_P$ — isobaric coefficient of thermal expansion, $B_T = -V(\partial P/\partial V)_T$ — isothermal elastic modulus. Previously, in [11,12,17], the activation parameters for these functions were calculated using the experimental temperature dependences obtained at $P = 0$. This made it possible to obtain temperature dependences of activation parameters at $P = 0$. But this method limited the $P-T$-range of activation parameter calculation.

Hereafter we used the expressions for functions Θ_o and γ_o obtained on the basis of a pairwise Mie–Lennard-Jones potential of interatomic interaction, which is as follows [18]:

$$\varphi(r) = \frac{D}{(b-a)}\left[a\left(\frac{r_o}{r}\right)^b - b\left(\frac{r_o}{r}\right)^a\right], \qquad (33)$$

where D and r_o — depth and coordinate of the potential minimum, $b > a > 1$ — parameters.

Then, as shown in [12,24], Debye temperature within the framework of the „only nearest neighbors interaction“ approximation can be determined as follows

$$\Theta_o(k_n^o, c_o) = A_w(k_n, c_o)\xi \times \left[-1 + \left(1 + \frac{8D}{k_B A_w(k_n^o, c_o)\xi^2}\right)^{1/2}\right], \qquad (34)$$

where function $A_w(k_n^o, c_o)$ arises due to the consideration of energy of „zero vibrations“ of atoms in a crystal

$$A_w(k_n^o, c_o) = K_R \cdot \frac{5k_n^o a b(b+1)}{144(b-a)}\left(\frac{r_o}{c_o}\right)^{b+2},$$

$$K_R = \frac{\hbar^2}{k_B r_o^2 m}, \quad \xi = \frac{9}{k_n^o}. \qquad (35)$$

From (34) the expressions can be found for the first (γ_o), second (q_o) and third (z_o) Grüneisen parameters. Their form is as follows:

$$\gamma_o = -\left(\frac{\partial \ln \Theta_o}{\partial \ln V}\right)_T = \frac{b+2}{6(1+X_w)},$$

$$q_o = \left(\frac{\partial \ln \gamma_o}{\partial \ln V}\right)_T = \gamma_o \cdot \frac{X_w(1+2X_w)}{(1+2X_w)},$$

$$z_o = -\left(\frac{\partial \ln q_o}{\partial \ln V}\right)_T = \gamma_o(1+4X_w) - 2q_o$$

$$= \gamma_o \cdot \left(\frac{1+3X_w}{1+X_w}\right) = \frac{(b+2)(1+3X_w)}{6(1+X_w)^2}, \qquad (36)$$

where function $X_w = A_w\xi/\Theta_o$ is introduced to define the role of quantum effects.

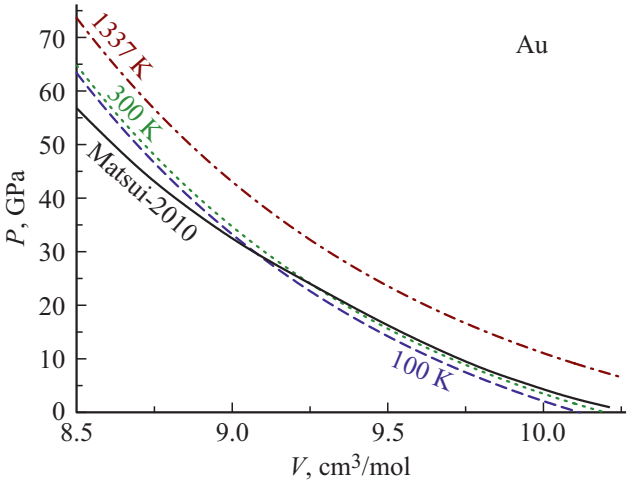

Figure 1. Isotherms of the gold state equation. The solid curve is the experimental dependence for $T = 300$ K from [29]. The other curves show the results of our calculations: the bottom dashed curve — for $T = 100$ K, the middle dotted curve — at $T = 300$ K, the top dashed-dotted curve — at $T = 1337$ K.

We used expressions (33)–(35) in papers [20,25] to study the change of activation parameters' energy characteristics under isothermal compression of the crystal volume: $V/V_0 = (c_o/r_o)^3$, up to $V/V_0 \cong 0$. Here, according to (2) and (33): $V = N[\pi/(6k_p)]c_o^3$ — crystal volume at $P-T$-arguments, $V_0 = N[\pi/(6k_p)]r_o^3$ — crystal volume at $P = 0$ and $T = 0$ K.

The study of the dependence of all activation parameters on $P-T$-arguments asked for an additional method, allowing to calculate both the state equation $P(T, V)$ and functions $\alpha_P(T, P)$ and $B_T(T, P)$, based on the interatomic potential parameters (33). Moreover, it was necessary to self-consistently determine all four interatomic potential parameters within the framework of the given calculation method (33). These tasks were solved in [26–28] where we developed an analytical method for calculating the properties of a single-component crystal containing no vacancies and delocalized atoms. Based on this method, the interatomic potential parameters were determined in [28] for 15 single-component metals.

In the present paper we used the method from [26–28] to calculate the properties of gold (Au, $m(\text{Au}) = 196.967$ a.m.u., $T_m(P = 0) = 1337.58$ K) which has a face-centered cubic (FCC) structure ($k_n^o = 12$, $k_p = 0.7405$). Gold is a low-oxidizable, inert and plastic metal which experiences no polymorphic phase transitions. The parameters of pairwise interatomic potential for FCC-Au (33) were determined in [28], and have the following values:

$$r_o = 2.8700 \cdot 10^{-10}\,\text{m}, \quad D/k_B = 7446.04\,\text{K},$$
$$b = 15.75, \quad a = 2.79. \qquad (37)$$

Fig. 1 shows the isothermal dependences of the state equation on volume $P(T, V)$ for gold. Fig. 2–4 shows

the isobaric temperature dependences of various properties of FCC-Au: Fig. 2 shows the dependence for elastic modulus $B_T(P, T)$, Fig. 3 — for thermal expansion coefficient $\alpha_P(P, T)$, Fig. 4 — for isobaric heat capacity: $C_p(P, T) = C_v(1 + \gamma\,\alpha_P T)$, where C_v is isochoric heat capacity.

As seen from Fig. 1–4, the suggested method makes it possible to obtain correct isobaric temperature dependences of gold properties both at $P = 0$ and at 24 GPa. The good agreement with the experimental dependences for gold at $P = 0$, shown in Fig. 1–4, indicates a very small contribution of vacancies and delocalization of atoms to the temperature dependences of the specified properties at $P = 0$. As shown in [20,25], the contribution of activation processes to the crystal lattice properties under an isothermal pressure rise decreases even more considerably. Along with that, as shown in [21,22], activation processes are accountable for such effects as crystal sublimation and melting, particularly at high pressures.

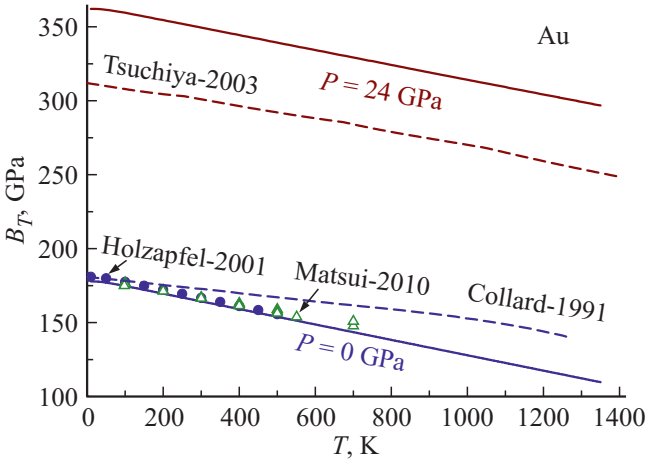

Figure 2. Isobaric dependences of the isothermal elastic modulus of gold on temperature. The bottom and top solid lines show our calculations at $P = 0$ and 24 GPa respectively. The symbols show the experimental data at $P = 0$: solid circles — the data from [30], the open triangles — the data from [29]. The bottom dashed line shows the experimental dependence from [31], the top dashed line shows the theoretical dependence obtained at $P = 24$ GPa in [32].

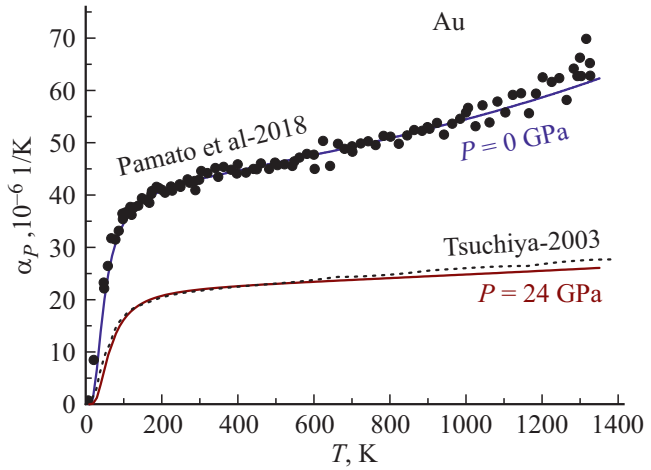

Figure 3. Isobaric dependences of the gold thermal expansion coefficient on temperature. The top and bottom solid lines show our calculations at $P = 0$ and 24 GPa respectively. The solid circles show the experimental data at $P = 0$ from [33]. The dashed line merging with the bottom solid line shows the theoretical dependence obtained at $P = 24$ GPa in [32].

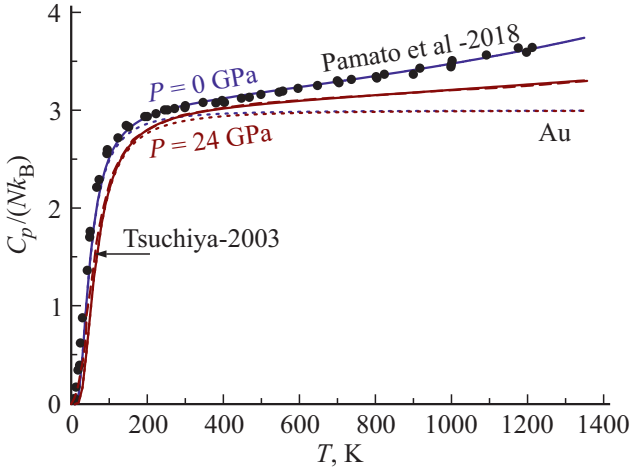

Figure 4. Isobaric dependences of normalized isobaric heat capacity of gold on temperature. The top and bottom solid lines show our calculations at $P = 0$ and 24 GPa respectively. The solid circles show the experimental data at $P = 0$ from [33]. The dashed line merging with the bottom solid line shows the theoretical dependence obtained at $P = 24$ GPa in [32]. The thin dotted lines show our calculated dependences for $C_v/(Nk_B)$ — the normalized isochoric heat capacity at $P = 0$ and 24 GPa respectively, which according to the Dulong–Petit law merge at high temperatures into the line $C_v/(Nk_B) = 3$.

7. Temperature and baric dependence of activation parameters

Temperature dependence of activation parameters for gold was calculated from 10 K to 1330 K along two isobars: $P = 0$ and 24 GPa. Curves *1–6* in Fig. 5 show the calculated isobaric dependences on reciprocal temperature for the activation parameters of gold. Curves *1* and *2* shows the logarithm of vacancy formation probability (10), curves *3* and *4* show the logarithm of atom delocalization (15), curves *5* and *6* show the logarithm of self-diffusion coefficient (29). The solid curves *1, 3, 5* are isobars of $P = 0$, the dashed curves *2, 4, 6* are isobars of $P = 24$ GPa. The dashed-dotted straight line *7* shows two experimental dependences for the self-diffusion coefficient logarithm obtained at $P = 0$ using the Arrhenius equation (32) at the temperature range of

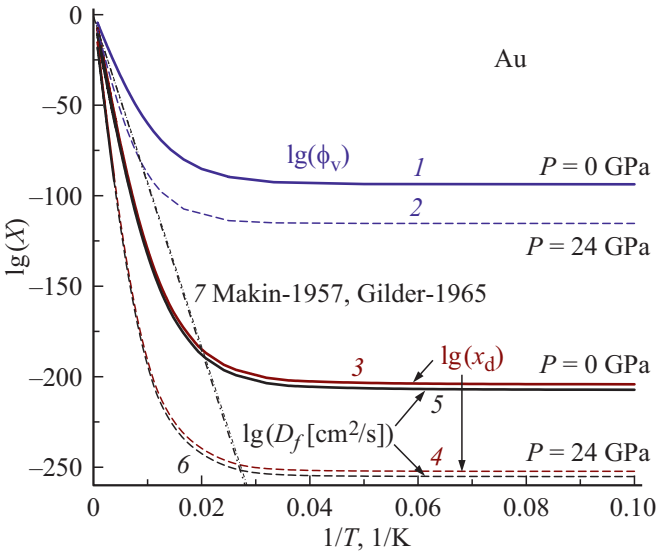

Figure 5. Isobaric dependences on reciprocal temperature for the activation parameters of gold. Curves *1* and *2* shows the calculation of the logarithm of vacancy formation probability (10), curves *3* and *4* show the calculation of the logarithm of atom delocalization (15), curves *5* and *6* show the calculation of the logarithm of self-diffusion coefficient (29). The solid curves *1, 3, 5* are isobars of $P = 0$, the dashed curves *2, 4, 6* are isobars of $P = 24$ GPa. The dashed-dotted straight line *7* shows the experimental dependences for the self-diffusion coefficient logarithm obtained at $P = 0$ in [34,35].

600 to 1320 K in [34,35] with the following parameters:

$$D_o = 0.091 \pm 0.001\,\mathrm{cm}^2/\mathrm{s}, \quad h_d = 1.81 \pm 0.01\,\mathrm{eV}, \ [34],$$

$$D_o = 0.107 \pm 0.002\,\mathrm{cm}^2/\mathrm{s}, \quad h_d = 1.834 \pm 0.002\,\mathrm{eV}\ [35].$$

These dependences in the scale of Fig. 5 merge into line *7*.

It can be seen from Fig. 5 that our dependence *5* at high temperatures for function $\lg(D_f/[\mathrm{cm}^2/\mathrm{s}])$ is somewhat steeper than the experimental straight line *7*. This is due to the fact that our dependence *5* was calculated for a perfect crystal, while dependence *7* was measured for a real crystal that contains both dislocations and grain boundaries which considerably increase the self-diffusion coefficient at high temperatures. For this reason, papers [36,37] suggested presenting the experimental self-diffusion coefficient as two terms:

$$D_f = D_{\mathrm{perf}} + D_{\mathrm{def}}, \tag{38}$$

where D_{perf} is the coefficient of self-diffusion in the lattice of a „perfect“ crystal, D_{def} is the coefficient of self-diffusion across defective places: across dislocations, across grain boundaries etc.

Fig. 6–9 shows the temperature dependences for thermodynamic parameters of activation processes calculated using formulas (20)–(23): Gibbs energy (g_i), enthalpy ($h_i = g_i + Ts_i$), entropy (s_i) and volume (v_i) of an activation process. The calculations were performed at $P = 0$ (solid curves *1, 3, 5*) and at $P = 24$ GPa (dashed curves *2, 4, 6*).

Along with the parameters of self-diffusion ($i = \mathrm{d}$, curves *3* and *4*) and the vacancy formation process ($i = \mathrm{v}$, curves *1* and *2*), we also calculated the thermodynamic parameters of migration ($i = \mathrm{m}$, curves *5* and *6*). They were determined as the difference between self-diffusion parameters and the corresponding parameters for vacancy formation [1,4]:

$$g_\mathrm{m} = g_\mathrm{d} - g_\mathrm{v}, \quad h_\mathrm{m} = h_\mathrm{d} - h_\mathrm{v},$$
$$s_\mathrm{m} = s_\mathrm{d} - s_\mathrm{v}, \quad v_\mathrm{m} = v_\mathrm{d} - v_\mathrm{v}. \tag{39}$$

The dashed-dotted straight lines *7* in Fig. 6 and 7 show the temperature dependences of Gibbs energy g_v and

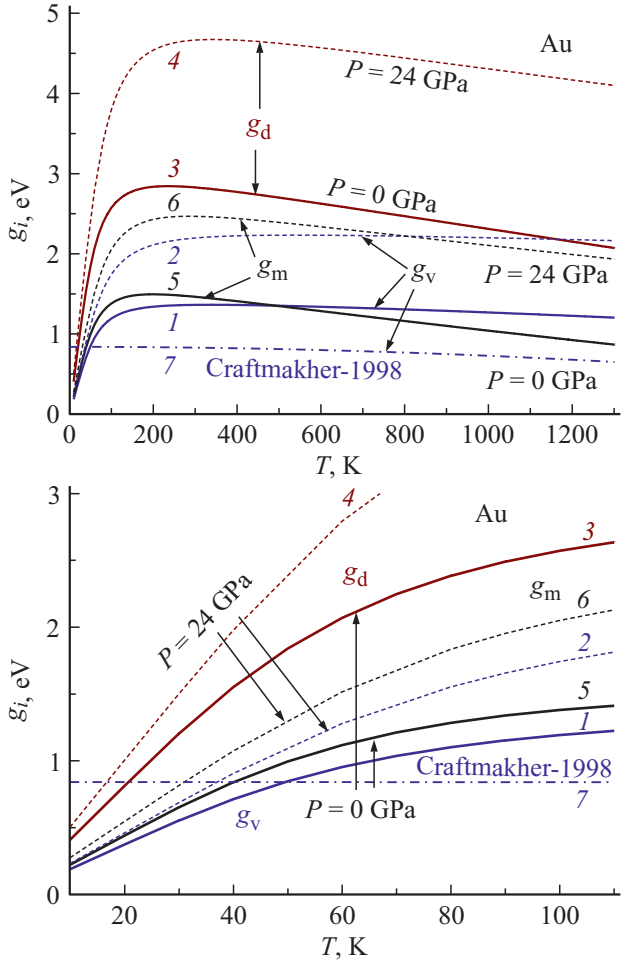

Figure 6. Temperature dependences of activation process Gibbs energy for gold. Curves *1* and *2* show the calculation of Gibbs energy for vacancy formation (21), curves *3* and *4* show the calculation of Gibbs energy for atom delocalization (22), curves *5* and *6* show the calculation of Gibbs energy for atom migration (39). The solid curves *1, 3, 5* are isobars of $P = 0$, the dashed curves *2, 4, 6* are isobars of $P = 24$ GPa. The dashed-dotted straight line *7* shows dependence (40) from [1, p. 164]. The top plot shows dependences $g_i(T)$ for the whole temperature region, the bottom plot — for the region of low temperatures ($i = \mathrm{v}, \mathrm{d}, \mathrm{m}$).

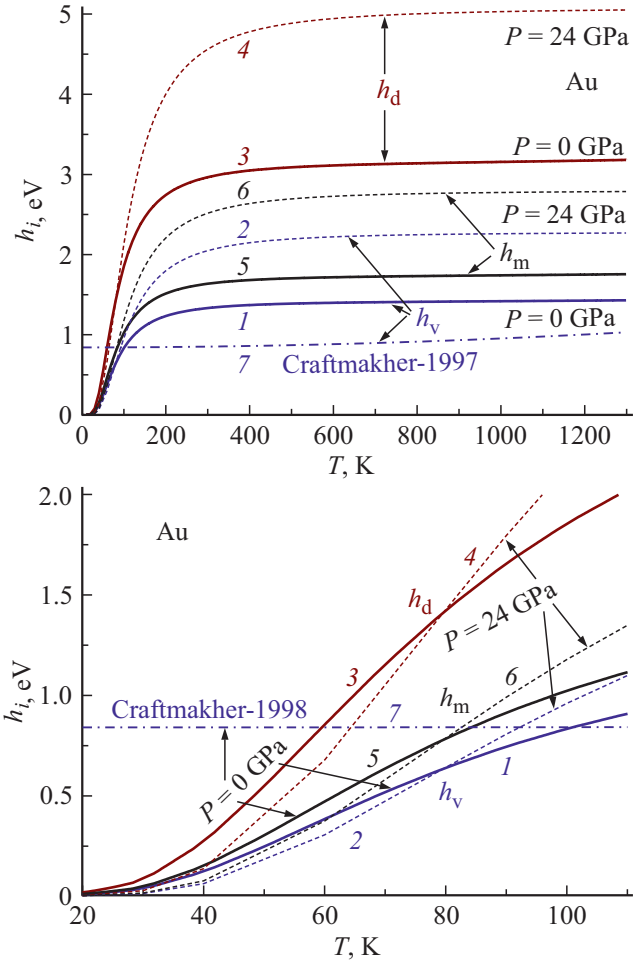

Figure 7. Temperature dependences of activation process enthalpy for gold. Curves *1* and *2* show the calculation of vacancy formation enthalpy (21), curves *3* and *4* show the calculation of atom delocalization enthalpy (22), curves *5* and *6* show the calculation of atom migration enthalpy (39). The solid curves *1, 3, 5* are isobars of $P = 0$, the dashed curves *2, 4, 6* are isobars of $P = 24$ GPa. The dashed-dotted straight line *7* shows dependence (40) from [1, p. 164]. The top plot shows dependences $h_i(T)$ for the whole temperature region, the bottom plot — for the region of low temperatures ($i = \mathrm{v},\ \mathrm{d},\ \mathrm{m}$).

enthalpy h_v for the vacancy formation process of form

$$g_\mathrm{v},\ \mathrm{eV} = 0.84 - 0.2\left(\frac{T}{T_\mathrm{m}}\right)^2,$$

$$h_\mathrm{v},\ \mathrm{eV} = 0.84 + 0.2\left(\frac{T}{T_\mathrm{m}}\right)^2. \qquad (40)$$

Dependences (40) were plotted in [1, p. 164], as per the experimental data for h_v obtained at $P = 0$, on the temperature range of 600 to 1320 K.

Fig. 6 shows that $g_i(P, T = 0\,\mathrm{K}) = 0$, and all the isobaric dependences $g_i(T)$ have the maxima which shift towards higher temperatures with a pressure rise. The following inequalities are fulfilled in the whole temperature range

$$g_\mathrm{d}(P, T) > g_\mathrm{m}(P, T) \quad \text{and} \quad g_\mathrm{d}(P, T) > g_\mathrm{v}(P, T).$$

But dependences $g_\mathrm{m}(P, T)$ and $g_\mathrm{v}(P, T)$ have an intersection point which shifts towards higher temperature with pressure rise. All three functions $g_i(T)$ in the region of high temperatures linearly decrease with temperature rise. Under isothermal pressure rise, all three Gibbs energies of the activation process rise in the whole temperature range.

It can be seen from Fig. 7 that all isobaric dependences $h_i(T)$ increase monotonically, while $h_i(P, T = 0\,\mathrm{K}) = 0$. The following inequalities are fulfilled in the whole temperature range:

$$h_\mathrm{d}(P, T) > h_\mathrm{m}(P, T) > h_\mathrm{v}(P, T). \qquad (41)$$

Under isothermal pressure rise, activation process enthalpy increases at high temperatures, which is physically clear. However, as seen from the bottom plot in Fig. 7, below a certain temperature (which is individual for the vacancy formation and self-diffusion process), activation process enthalpy decreases under isothermal compression. This is conditioned by a temperature-baric dependence of activation process entropy in the function: $h_i = g_i + Ts_i$.

Activation process enthalpy is the only measurable parameter from the 4 which characterize the activation process. However, h_i was determined experimentally only at high temperatures ($T \gg \Theta$), where activation processes exert the maximum impact on crystal properties and, therefore, quantity h_i can be estimated experimentally. Thereat, an exponential Arrhenius dependence of type (32) is used and it is assumed that activation process enthalpy does not depend on temperature.

Enthalpies of vacancy formation and self-diffusion for gold were measured at $P = 0$ in the temperature range of 600 to 1320 K by different methods. They are within

$$h_\mathrm{v}(T \gg \Theta) = 0.89{-}1.02\,\mathrm{eV}\ [1],$$

$$h_\mathrm{d}(T \gg \Theta) = 1.71{-}1.833\,\mathrm{eV}\ [5]. \qquad (42)$$

Our data for the given temperature range exceeds the experimental estimates. This can be due both to the difference of our model of a defect-free crystal from the real crystal and due to the approximation of our calculations, based only on 4 parameters (37) for the pairwise potential of interatomic interaction (33).

Along with that, the modern computer modeling methods (first-principles density functional theory — DFT, embedded-atom method — EAM, etc.) made it possible to calculate the vacancy formation enthalpy only at $T = 0$ K and at an indefinite pressure. The following values were

obtained for gold using these methods [38]:

$h_v(T = 0\,\mathrm{K})$, eV = 0.42–0.67 (DFT-PBE (Perdew, Burke, Ernzerhof)) — 0.62–0.72 (DFT-LDA (local density approximation)) — 0.71(EAM and LSGF (locally self-consistent Green's-function)) — 0.72 (DFT-HSE (Heyd, Scuseria, Ernzerhof)) — 0.82 (FP-LMTO (full potential linear muffin-tin orbital)) — 1.24 (TB (tight-binding method)).

In [39] the above-mentioned DFT-methods of computer modeling were complemented with Posteriori surface error correction, which made the results of the DFT-methods closer to the experimental quantity $h_v(T \gg \Theta)$ from (42):

$h_v(T = 0\,\mathrm{K})$, eV = 0.84 (DFT-LDA)–0.87 (DFT-PBE) — 0.92 (DFT-revTPSS (Tao, Perdew, Staroverov, Scuseria)) — 1.01 (DFT-PW91 (Perdew, Wang)).

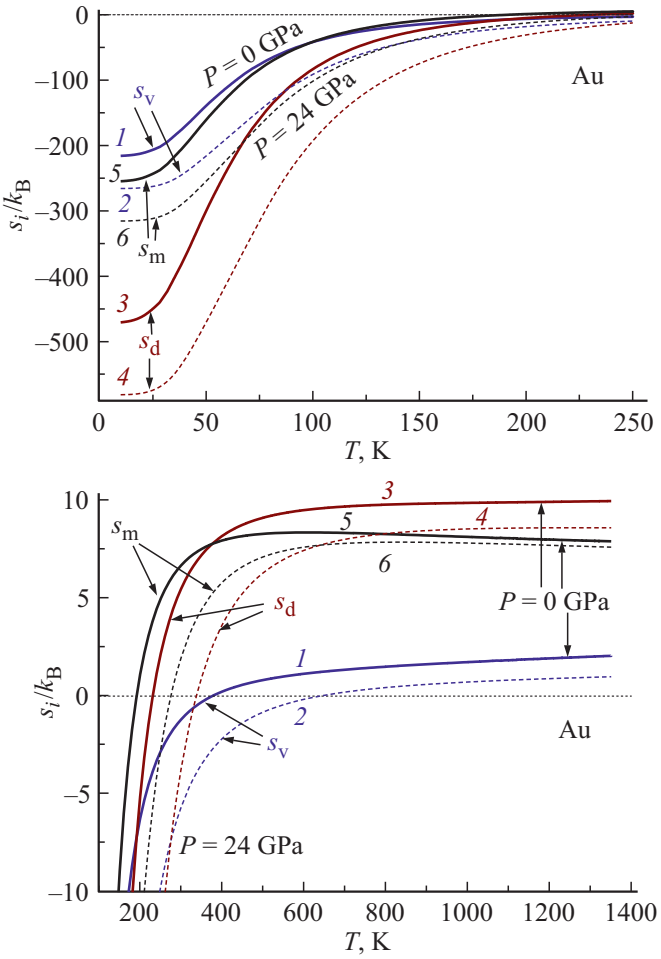

Figure 8. Temperature dependences of activation process entropy calculated for gold. Curves *1* and *2* — vacancy formation entropy from (21), curves *3* and *4* — atom delocalization entropy from (22), curves *5* and *6* — atom migration entropy from (39). The solid curves *1, 3, 5* are isobars of $P = 0$, the dashed curves *2, 4, 6* are isobars of $P = 24$ GPa. The top plot shows dependences $s_i(T) < 0$ in the region of low temperatures, the bottom plot — for the region of high temperatures (i = v, d, m).

Fig. 8 shows that all isobaric dependences $s_i(T)$ at low temperatures are in the negative region, and the following relations are fulfilled

$$s_d(P, T = 0\,\mathrm{K}) < s_m(P, T = 0\,\mathrm{K}) < s_v(P, T = 0\,\mathrm{K}) < 0. \quad (43)$$

However, these relations in the region of high temperatures change to the following form:

$$s_d(P, T \gg \Theta) > s_m(P, T \gg \Theta) > s_v(P, T \gg \Theta) > 0. \quad (44)$$

Under isothermal pressure rise, activation process entropy decreases in the whole temperature range.

It should be noted that nowadays there are still no experimental or theoretical methods for correct estimation not only of temperature dependence $s_i(T)$, but even the magnitude of activation process entropy at $P = 0$ and $T \gg \Theta$ [8,9,33,40]. In this respect, the literature gives different indirect estimates for $s_i(T \gg \Theta)$, which are all positive but considerably different. For instance, the following values of vacancy formation entropy are used for gold:

$$s_v(T \gg \Theta)/k_B = 3.15\ [1, \text{p. } 164],\quad 0.5\ [19],$$

$$1.03\text{–}1.26\ [33],\quad 0.5\text{–}3.1\ [41],\quad 0.5\text{–}0.7\ [42].$$

We have still not found in the literature any experimental or theoretical estimates of quantity $s_d(T \gg \Theta)$ for gold.

It can be seen from Fig. 9 that all isobaric dependences $v_i(T)$ increase monotonically with temperature rise, while $v_i(P, T = 0\,\mathrm{K}) = 0$. In our calculations we adopted $v_0 = \pi \cdot r_o^3/(6k_p)$ is atom volume in a perfect crystal at $P = 0$ and $T = 0\,\mathrm{K}$. It can be seen from Fig. 9 that the following relation is fulfilled in the whole temperature range:

$$v_d(P, T) > v_m(P, T) > v_v(P, T) > 0. \quad (45)$$

Experimental deviation of activation process volume is a very labor-intensive process, while theoretical estimates for v_i are very approximate [43,44]. The literature reports the following estimates for the normalized value of gold activation volume (the theoretical estimates are given in brackets):

$$v_v(T \gg \Theta)/v_0 = (0.63\text{–}0.73),\quad 0.52\ [1, \text{p. } 92];$$

$$0.50\text{–}0.59\ [7];\quad 0.52\text{–}0.65\ [33, 44];$$

$$(0.35\text{–}0.48),\quad 0.45\text{–}0.59\ [42];\quad 0.45\text{–}0.57\ [43];$$

$$0.3\text{–}0.5(\text{at } T < \Theta),\ 0.5\text{–}0.7(\text{at } T > \Theta)\ [45];$$

(0.73), 0.52–0.85 [46]; (0.73), 0.85 [47];

$v_d(T \gg \Theta)/v_0 = 0.706$ [2]: 0.65–0.90 [7];

0.60–0.72 [43]; 0.73–0.77 [48].

Fig. 9 shows that the activation process volume decreases under isothermal compression. A decrease of vacancy formation volume under isothermal compression was also noted in [49] for BCC-Ta and in [50] for FCC-Au, as follows:

$$v_d(T = 953\,\mathrm{K})/v_0 = 0.65 \quad \text{at} \quad P = 0.6\,\mathrm{GPa},$$

$$0.53 \quad \text{at} \quad P = 1.1\,\mathrm{GPa}.$$

Moreover, the authors of [42,51] obtained the relation $v_v(T \gg \Theta) \approx 8\Delta v_m$ for single-component metals, where Δv_m is specific volume leap during melting. Since quantity Δv_m decreases with pressure rise, this relation also indicates a decrease of quantity $v_v(T \gg \Theta)$ with pressure rise.

8. Behavior of activation parameters at low temperatures

At $T \ll \Theta$ — the functions $f_y(T)$ and $t_y(T)$ from (7) and (23) considerably vary with temperature, and the following limit relations are fulfilled:

$$f_y(T = 0\,\mathrm{K}) = \lim_{\frac{T}{\Theta_0}\to 0} f_y\left(\frac{\Theta_0}{T}\right) = \frac{8}{3}\lim_{\frac{T}{\Theta_0}\to 0}\left(\frac{T}{\Theta_0}\right) = 0. \tag{46}$$

$$t_y(T = 0\,\mathrm{K}) = \lim_{\frac{T}{\Theta_0}\to 0} t_y\left(\frac{\Theta_0}{T}\right)$$

$$= 1 - \frac{6}{4}\lim_{\frac{T}{\Theta_0}\to 0}\left(\frac{\Theta_0}{T}\right)\exp\left(-\frac{3\Theta_0}{4T}\right) = 1, \tag{47}$$

where $\Theta_0 = \Theta_o(T = 0\,\mathrm{K})$ is the Debye temperature calculated for a defect-free crystal at $T = 0\,\mathrm{K}$.

Given the fact that the following is true at low temperatures: $\alpha_P(T) \sim T^3$ [14,18,19] (i.e. we have: $\alpha_P(0) = 0$), formulas (3) and (15) provide the following expressions for the activation process probability at $T = 0\,\mathrm{K}$ [12,23,52]:

$$\phi_v(0) = \frac{N_v(0)}{N + N_v(0)} = \frac{2}{\pi^{1/2}}\int\limits_{(M_v)^{1/2}}^{\infty}\exp(-t^2)dt$$

$$\cong \frac{1}{(\pi M_v)^{1/2}}\exp(-M_v), \tag{48}$$

$$x_d(0) = \frac{N_d(0)}{N} = \frac{2}{\pi^{1/2}}\int\limits_{M_d}^{\infty} t^{1/2}\exp(-t)dt$$

$$\cong 2\left(\frac{M_d}{\pi}\right)^{1/2}\exp(M_d), \tag{49}$$

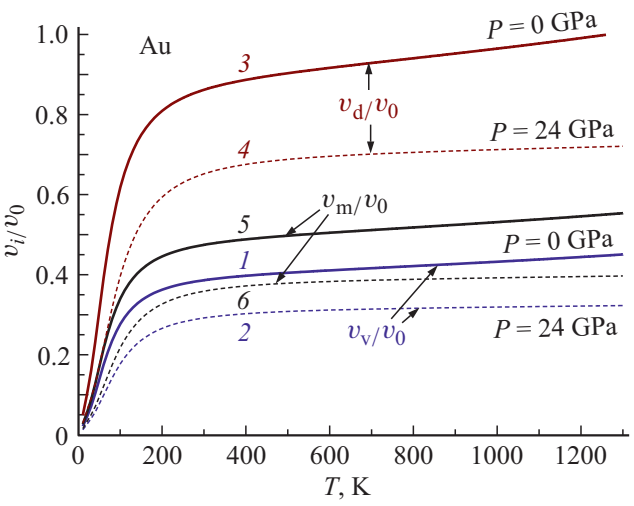

Figure 9. Temperature dependences of activation process volume (normalized to the atom volume) calculated for gold. Curves *1* and *2* show the calculation of vacancy formation volume as per (21), curves *3* and *4* show the calculation of atom delocalization volume as per (22), curves *5* and *6* show the calculation of atom migration volume as per (39). The solid curves *1, 3, 5* are isobars of $P = 0$, the dashed curves *2, 4, 6* are isobars of $P = 24\,\mathrm{GPa}$ (i = v, d, m).

where parameters M_v and M_d represent the following limit relations

$$M_v = \lim_{\frac{T}{\Theta_0}\to 0}\left(\frac{E_v}{k_B T}\right) = \frac{M_L}{1 + x_d(0)(C_D M_L - 1)}, \tag{50}$$

$$M_d = \lim_{\frac{T}{\Theta_0}\to 0}\left(\frac{E_d}{k_B T}\right) = \frac{8E_{d1}(0)}{3k_B\Theta_0} = C_{LD}M_L. \tag{51}$$

The following notations are introduced here:

$$M_L = \lim_{\frac{T}{\Theta_0}\to 0}\left(\frac{E_L}{k_B T}\right) = \frac{8E_{L1}(0)}{3k_B\Theta_0} = \frac{3mk_B\Theta_0}{8k_n^o}\left[\frac{c_o(0)}{\hbar}\right]^2,$$

$$E_{L1}(0) = E_L(T = 0\,\mathrm{K},\ f_y = 1) = \frac{m}{k_n^o}\left[\frac{3c_o(0)k_B\Theta_0}{8\hbar}\right]^2,$$

$$E_{d1}(0) = E_d(T = 0\,\mathrm{K},\ f_y = 1) = \frac{27m}{128k_p^{2/3}}\left[\frac{c_o(0)k_B\Theta_0}{\pi\hbar}\right]^2. \tag{52}$$

Thus, at $T = 0\,\mathrm{K}$ the crystal has „zero vacancies“, while the self-diffusion coefficient is non-zero: $\phi_v(0) > 0$ and $x_d(0) > 0$. This effect occurs because the atoms have „zero vibrations“ and was predicted by Andreev and Lifshitz in 1969 [53,54]. Accordingly, the activation Arrhenius formula with temperature-independent activation energy at low temperature cannot be applied to describe activation processes.

The following limit relations are obtained for thermodynamic parameters of activation processes at $T = 0\,\mathrm{K}$ [12,23,52]:

for the vacancy formation process

$$\lim_{\frac{T}{\Theta_0}\to 0}\left(\frac{g_\mathrm{v}}{k_\mathrm{B}T}\right)=M_\mathrm{v}+0.5\ln(\pi M_\mathrm{v}),\quad \lim_{\frac{T}{\Theta_0}\to 0}\left(\frac{h_\mathrm{v}}{k_\mathrm{B}T}\right)=0,$$

$$\lim_{\frac{T}{\Theta_0}\to 0}\left(\frac{s_\mathrm{v}}{k_\mathrm{B}}\right)=\frac{s_\mathrm{v}(0)}{k_\mathrm{B}}=-M_\mathrm{v}-0.5\ln(\pi M_\mathrm{v}),$$

$$\lim_{\frac{T}{\Theta_0}\to 0}\left(\frac{v_\mathrm{v}}{v_\mathrm{a}}\right)=\frac{v_\mathrm{v}(0)}{v_\mathrm{a}(0)}=0,$$

$$\lim_{\frac{T}{\Theta_0}\to 0}\left(\frac{v_\mathrm{v}B_T}{k_\mathrm{B}T}\right)=\phi_{E0}\left[\gamma_\mathrm{o}(0)-\frac{2}{3}\right]$$

$$=M_\mathrm{v}[1+x_\mathrm{d}(0)C_\mathrm{D}M_\mathrm{v}M_\mathrm{d}G_{\mathrm{d}0}]\cdot\left[\gamma_\mathrm{o}(0)-\frac{2}{3}\right],$$

$$\phi_{E0}=M_\mathrm{v}[1+x_\mathrm{d}C_\mathrm{D}M_\mathrm{v}M_\mathrm{d}G_{\mathrm{d}0}],$$

$$G_{\mathrm{d}0}=1-\frac{1}{C_\mathrm{D}M_\mathrm{L}}-\frac{1}{M_\mathrm{d}}. \qquad (53)$$

for the self-diffusion process

$$D_f(0)=D_\mathrm{d}(\rho)_0\cdot x_\mathrm{d}(0),\quad D_\mathrm{d}(\rho)_0=f_\mathrm{cor}\cdot\frac{k_\mathrm{B}\Theta_\mathrm{o}c_\mathrm{o}(0)^2}{2\pi^2\hbar k_\mathrm{p}^{2/3}},$$

$$\lim_{\frac{T}{\Theta_0}\to 0}\left(\frac{g_\mathrm{d}}{k_\mathrm{B}}\right)=M_\mathrm{d}-0.5\ln\left(\frac{4M_\mathrm{d}}{\pi}\right),\quad \lim_{\frac{T}{\Theta_0}\to 0}\left(\frac{h_\mathrm{d}}{k_\mathrm{B}T}\right)=0,$$

$$\lim_{\frac{T}{\Theta_0}\to 0}\left(\frac{s_\mathrm{d}}{k_\mathrm{B}}\right)=\frac{s_\mathrm{d}(0)}{k_\mathrm{B}}=-M_\mathrm{d}+0.5\ln\left(\frac{4M_\mathrm{d}}{\pi}\right),$$

$$\lim_{\frac{T}{\Theta_0}\to 0}\left(\frac{v_\mathrm{d}}{v_\mathrm{a}}\right)=\frac{v_\mathrm{d}(0)}{v_\mathrm{a}(0)}=0,$$

$$\lim_{\frac{T}{\Theta_0}\to 0}\left(\frac{v_\mathrm{d}B_T}{k_\mathrm{B}T}\right)=M_\mathrm{d}\cdot\left[\gamma_\mathrm{o}(0)-\frac{2}{3}\right]. \qquad (54)$$

It follows from formulas (21) and (22) that functions $s_\mathrm{v}(T)$ and $s_\mathrm{d}(T)$ are positive only under the following conditions [55]:

$$\left(\frac{k_\mathrm{B}T}{2E_\mathrm{L}}\right)\ln\left(\frac{\pi E_\mathrm{L}}{k_\mathrm{B}T}\right)+\alpha_P T\left[(2-t_y)\gamma_\mathrm{o}-\frac{2}{3}\right]\geq t_y, \qquad (55)$$

$$\left(\frac{k_\mathrm{B}T}{2E_\mathrm{d}}\right)\ln\left(\frac{4E_\mathrm{d}}{\pi k_\mathrm{B}T}\right)+\alpha_P T\left[(2-t_y)\gamma_\mathrm{o}-\frac{2}{3}\right]\geq t_y, \qquad (56)$$

Since inequality $E_\mathrm{d}/E_\mathrm{L}=C_\mathrm{LD}=3k_n^\mathrm{o}/(2\pi^2k_\mathrm{p}^{2/3})>1$ is fulfilled, the equality in condition (56) is achieved at a lower temperature ($T_{s\mathrm{d}=0}$) than in condition (55) for positivity of vacancy formation entropy. Thus, the following inequality is fulfilled under isobaric heating: $T_{s\mathrm{v}=0}>T_{s\mathrm{d}=0}>0\,\mathrm{K}$.

It should be noted that Varotsos and Alexopoulos in 1979 showed in [56] that a negative value of vacancy formation entropy ($s_\mathrm{v}<0$) does not contradict the thermodynamic conditions of vacancy formation. A negative value of vacancy formation entropy at low temperatures was experimentally found in BCC- and HCP-modifications of ^{3}He and ^{4}He crystals in [57–61].

Paper [8] showed theoretically, by the example of aluminum, that vacancy formation entropy will be negative if vacancy formation enthalpy is considered as temperature-dependent. Paper [62], dealing with theoretical study of self-diffusion in BCC-Zr by the molecular dynamics method, showed that vacancy formation entropy at temperatures below 600 K becomes negative. Thus, our result of transition of the activation process entropy to the negative region at temperature decrease agrees with the experimental and theoretical papers of other authors who studied activation processes at low temperatures.

It should be noted that the presence of vacancies and D-atoms in a crystal at $T=0\,\mathrm{K}$ does not violate the third law of thermodynamics which states as follows: specific (per atom) crystal entropy at $T=0\,\mathrm{K}$ is equal to zero: $s(T=0\,\mathrm{K})=0$. It follows from the entropy definition that

$$s(T,P)=-\left(\frac{\partial g}{\partial T}\right)_P=-\left(\frac{\partial g}{\partial T}\right)_{P,x_\mathrm{d},\phi_\mathrm{v}}$$

$$-\left(\frac{\partial g}{\partial \phi_\mathrm{v}}\right)_P\left(\frac{\partial \phi_\mathrm{v}}{\partial T}\right)_P-\left(\frac{\partial g}{\partial x_\mathrm{d}}\right)_P\left(\frac{\partial x_\mathrm{d}}{\partial T}\right)_P. \qquad (57)$$

where $g(T,P)$ is specific (per atom) free Gibbs energy of a crystal.

The first term in (57) is crystal entropy (per atom) arising due to a temperature change while the share of activation parameters remains unchanged. The first term in (57) in case of the Einstein crystal model decreases at $T\to 0\,\mathrm{K}$ in proportion to the dependence [14,18,19]: $\exp(-\Theta/T)$. The second and third terms in (57) are contributions to entropy (per atom) arising only due to a change in concentration of vacancies and D-atoms in a crystal. As clearly seen from Fig. 5, at $T=0\,\mathrm{K}$ functions $\phi_\mathrm{v}(T)$ and $x_\mathrm{d}(T)$ have their minima. Therefore, the third and second terms in (57) at $T=0\,\mathrm{K}$ also disappear.

Since the activation process volume at $T=0\,\mathrm{K}$ is equal to zero, the presence of vacancies and D-atoms at $T=0\,\mathrm{K}$ does not affect the crystal thermal expansion coefficient.

Since functions $s_\mathrm{d}(T)$ and $s_\mathrm{v}(T)$ have a negative value at $0\,\mathrm{K}<T<T_{s\mathrm{d}=0}<T_{s\mathrm{v}=0}$, here heat equal to Ts_v or Ts_d respectively is emitted under isobaric formation of a vacancy or a D-atom in a crystal. This agrees with the conclusion made in [53,54]: at $T=0\,\mathrm{K}$, it more profitable (from the energy viewpoint) for a crystal to go over to a state in which a part of the lattice nodes is vacant, while a part of the atoms diffuse across the crystal. Atom delocalization and vacancy formation at $0<T<T_{s\mathrm{d}=0}<T_{s\mathrm{v}=0}$ lead to „ordering“ of the crystal lattice. It should be noted that this property is not a prerogative of quantum crystal. It is inherent in all substances, but is most noticeable in ^{3}He and ^{4}He crystals, due to a relatively large amplitude of „zero vibrations“ of atoms in these substances.

At high temperatures ($T/\Theta_\mathrm{Eo}>2$) we can adopt $f_y\cong 1$ and $t_y\cong 0$. Therefore, activation process entropy in this temperature region is always positive. Vacancies and

D-atoms forming under these conditions set the crystal to a more disordered state.

We would like to conclude by saying that the thermodynamic definitions of activation parameters (21) and (22) include two functions: α_P — thermal expansion coefficient and B_T — elastic modulus. These functions are inconvenient due to their peculiarities under a first-order phase transition (PT-I), e.g., in case of a crystal−liquid phase transition (C−L PT). Function $\alpha_P(T, V)$ in the binodal region of the S-loop of C−L PT has a discontinuity of type II, i.e. the function extends to infinity. Due to this, we obtain the following on the binodal of C−L PT: h_v, s_v, h_d and $s_\mathrm{d} \to \infty$. On the other hand, $B_T = 0$ is fulfilled at points of the spinodal of the S-loop of C−L PT, and $B_T < 0$ in the inter-spinodal region. Due to this, functions v_v and v_d at spinodal points have a discontinuity of type II: v_v and $v_\mathrm{d} \to \infty$, and v_v and $v_\mathrm{d} < 0$ the inter-spinodal region. In this respect, the apparatus of equilibrium and reversible thermodynamics is ineffective in the C−L PT region (as well as in the region of the binodal of the S-loop of any PT-I) as applied to activation process description: vacancy formation or self-diffusion. Therefore, it was impossible up to now to estimate the behavior of functions h_v, s_v, v_v, h_d, s_d and v_d in the region of C−L PT. In this sense, the method for calculation of functions $\phi_\mathrm{v}(P, T)$ and $x_\mathrm{d}(P, T)$ from expressions (10)−(19) has a wider application field. It was shown in [21,22], when calculating the argon phase diagram.

9. Conclusion

1. We developed an analytical method for calculating the dependence of activation parameters in a crystal of a single-component substance on pressure and temperature.

2. The method was tried for a FCC-crystal of gold in calculations of temperature dependence of activation parameters along two isobars: $P = 0$ and 24 GPa. The data agrees well with the experimental and theoretical estimates reported in literature.

3. It is shown that the temperature dependence of activation parameters at low temperatures ($T < \Theta$) is quite considerable due to quantum effects. The temperature dependence of activation parameters at high temperatures ($T > \Theta$) weakens and is almost linear.

4. It is shown that activation process entropy rises with temperature, passing from the region of negative values to the positive region at $T \gg \Theta$.

5. It is shown that the use of the Arrhenius equation for determination of energy parameters, both for vacancy formation and for self-diffusion, is incorrect at low temperatures. The use of the Arrhenius equation for gold is incorrect already at $T < 200$ K.

6. Gibbs energy increases under isothermal compression, while activation process entropy and volume decrease in the whole temperature range. Activation process enthalpy increases with pressure rise only at high temperatures, while below a certain temperature (which is individual for the vacancy formation and self-diffusion process), activation process enthalpy under isothermal compression decreases.

7. It is shown that the thermodynamic processes of the activation process at $T = 0$ K reach their minimum: Gibbs energy, enthalpy and volume of the activation process become zero, while the minimum of the activation process entropy lies in the negative region.

Acknowledgments

The author would like to thank S.P. Kramynin, K.N. Magomedov, N.Sh. Gazanova, Z.M. Surkhayeva and M.M. Gadzhieva for fruitful discussions and assistance in work.

Funding

The work has been funded by RFBR (grant No. 18-29-11013_mk).

Conflict of interest

The author declares that he has no conflict of interest.

References

[1] Y. Kraftmakher. Phys. Rep. **299**, *2−3*, 79 (1998). DOI: 10.1016/S0370-1573(97)00082-3
[2] J.R. Manning, Diffusion Kinetics for Atoms in Crystals. D. Van Nostrand Comp., Toronto (1968). 257 p.
[3] B.S. Bokshtein, A.B. Yaroslavtsev. Diffuziya atomov i ionov v tverdykh telakh. Izd-vo MISiS, M. (2005). 362 p. (in Russian).
[4] P.A. Varotsos, K.D. Alexopoulos. Thermodynamics of point defects and their relation with bulk properties. Elsevier, Amsterdam, North Holland (2013). 489 p.
[5] G. Neumann, C. Tuijn. Self-diffusion and impurity diffusion in pure metals: handbook of experimental data. Pergamon/Elsevier, Boston (2009). 349 p.
[6] C. Freysoldt, B. Grabowski, T. Hickel, J. Neugebauer, G. Kresse, A. Janotti, C.G. Van de Walle. First-principles calculations for point defects in solids. Rev. Mod. Phys. **86**, *1*, 253 (2014). DOI: 10.1103/RevModPhys.86.253
[7] H. Mehrer. The effect of pressure on diffusion. Defect and Diffusion Forum **129−130**, 57 (1996). DOI: 10.4028/www.scientific.net/DDF.129-130.57
[8] N.P. Kobelev, V.A. Khonik. J. Exp. Theor. Phys. **126**, *3*, 340 (2018). DOI: 10.1134/S1063776118030032
[9] G. Smirnov. Phys. Rev. B **102**, *18*, 184110 (2020). DOI: 10.1103/PhysRevB.102.184110
[10] P.-W. Ma, S.L. Dudarev. Phys. Rev. Mater. **3**, *6*, 063601 (2019). DOI: 10.1103/physrevmaterials.3.063601
[11] M.N. Magomedov. Semiconductors **42**, *10*, 1133 (2008). DOI: 10.1134/S1063782608100011
[12] M.N. Magomedov, Study of Interatomic Interaction, Vacancy Formation and Self-Diffusion in Crystals. Fizmatlit, Moscow (2010).
[13] Handbook of Mathematical Functions / Eds M. Abramowitz, I. Stegun. National Bureau of Standards, N.Y. (1964). 1046 p. https://www.math.hkbu.edu.hk/support/aands/intro.htm

[14] R.P. Feynman, Statistical Mechanics. W.A. Benjamin Inc., Massachusetts (1972). 354 p.
[15] A.G. Chirkov, A.G. Ponomarev, V.G. Chudinov. Tech. Phys. **49**, *2*, 203 (2004). DOI: 10.1134/1.1648956
[16] G.M. Poletaev, M.D. Starostenkov. Phys. Solid State **51**, *4*, 727 (2009). DOI: 10.1134/S106378340904012X
[17] M.N. Magomedov. Semiconductors **44**, *3*, 271 (2010). DOI: 10.1134/S1063782610030012
[18] E.A. Moelwyn-Hughes. Physical Chemistry. Pergamon Press, London (1961). 1333 p.
[19] L.A. Girifalco. Statistical Physics of Materials. J. Wiley & Sons Ltd, N. Y. (1973). 346 p.
[20] M.N. Magomedov. Phys. Met. Metallography **114**, *3*, 207 (2013). DOI: 10.1134/S0031918X13030113
[21] M.N. Magomedov. J. Mol. Liquids **285**, 106 (2019). DOI: 10.1016/j.molliq.2019.04.032
[22] M.N. Magomedov. Phys. Solid State **63**, *7*, 1111 (2021). DOI: 10.1134/S1063783421070167
[23] M.N. Magomedov. Tech. Phys. Lett. **28**, *5*, 430 (2002). DOI: 10.1134/1.1482758
[24] M.N. Magomedov. Tech. Phys. **58**, *9*, 1297 (2013). DOI: 10.1134/S106378421309020X
[25] M.N. Magomedov. Tech. Phys. **58**, *12*, 1789 (2013). DOI: 10.1134/S1063784213120153
[26] M.N. Magomedov. Phys. Solid State **63**, 215 (2021). DOI: 10.1134/S1063783421020165
[27] M.N. Magomedov. Phys. Solid State **62**, *7*, 1126 (2020). DOI: 10.1134/S1063783420070136
[28] M.N. Magomedov. Phys. Solid State **63**, *9*, 1595 (2021). DOI: 10.1134/S1063783421090250
[29] M. Matsui. J. Phys.: Conf. Ser. **215**, *1*, 012197 (2010). DOI: 10.1088/1742-6596/215/1/012197
[30] W.B. Holzapfel, M. Hartwig, W. Sievers. J. Phys. Chem. Reference Data **30**, *2*, 515 (2001). DOI: 10.1063/1.1370170
[31] S.M. Collard, R.B. Mc Lellan. Acta Metallurgica Mater. **39**, *12*, 3143 (1991). DOI: 10.1016/0956-7151(91)90048-6
[32] T. Tsuchiya. J. Geophys. Res. **108**, *B10*, 2462 (2003). DOI: 10.1029/2003JB002446
[33] M.G. Pamato, I.G. Wood, D.P. Dobson, S.A. Hunt, L. Vočadlo. J. Appl. Crystallogr. **51**, *2*, 470 (2018). DOI: 10.1107/S1600576718002248
[34] S.M. Makin, A.H. Rowe, A.D. Leclaire. Proc. Phys. Soc. Section B **70**, *6*, 545 (1957). DOI: 10.1088/0370-1301/70/6/301
[35] H.M. Gilder, D. Lazarus. J. Phys. Chem. Solids **26**, *12*, 2081 (1965). DOI: 10.1016/0022- 3697(65)90250-7
[36] E.W. Hart. Acta Metallurgica **5**, *10*, 597 (1957). DOI: 10.1016/0001-6160(57)90127-x
[37] H.M. Morrison, V.L.S. Yuen. Canadian J. Physics **49**, *21*, 2704 (1971). DOI: 10.1139/p71-326
[38] W. Xing, P. Liu, X. Cheng, H. Niu, H. Ma, D. Li, Y. Li, X.-Q. Chen. Phys. Rev. B **90**, *14*, 144105 (2014). DOI: 10.1103/PhysRevB.90.144105
[39] B. Medasani, M. Haranczyk, A. Canning, M. Asta. Comput. Mater. Sci. **101**, *C*, 96 (2015). DOI: 10.1016/j.commatsci.2015.01.018
[40] R.A. Konchakov, A.S. Makarov, A.S. Aronin, N.P. Kobelev, V.A. Khonik. J. Exp. Theor. Phys. Lett. **113**, *5*, 345 (2021). DOI: 10.1134/S0021364021050064
[41] P. Varotsos, K. Alexopoulos. Phys. Rev. B **15**, *8*, 4111 (1977). DOI: 10.1103/PhysRevB.15.4111
[42] W. Bollmann, N.F. Uvarov, E.F. Hairetdinov. Cryst. Res. Technol. **24**, *4*, 422 (1989). DOI: 10.1002/crat.2170240418
[43] R.H. Dickerson, R.C. Lowell, C.T. Tomizuka. Phys. Rev. **137**, *2A*, A613 (1965). DOI: 10.1103/physrev.137.a613
[44] R.M. Emrick. Phys. Rev. B **22**, *8*, 3563 (1980). DOI: 10.1103/PhysRevB.22.3563
[45] P. Varotsos, W. Ludwig, K. Alexopoulos. Phys. Rev. B **18**, *6*, 2683 (1978). DOI: 10.1103/PhysRevB.18.2683
[46] G.J. Ackland, G. Tichy, V. Vitek, M.W. Finnis. Phil. Mag. **A56**, *6*, 735 (1987). DOI: 10.1080/01418618708204485
[47] P.A. Korzhavyi, I.A. Abrikosov, B. Johansson, A. Ruban, H.L. Skriver. Phys. Rev. B **59**, *18*, 11693 (1999). DOI: 10.1103/PhysRevB.59.11693
[48] P. Knorr, J. Jun, W. Lojkowski, C. Herzig. Phys. Rev. B **57**, *1*, 334 (1998). DOI: 10.1103/physrevb.57.334
[49] S. Mukherjee, R.E. Cohen, O. Gülseren. J. Phys.: Condens. Matter **15**, *6*, 855 (2003). DOI: 10.1088/0953-8984/15/6/312
[50] M. Senoo, H. Mii, I. Fujishiro, T. Takeuchi. Jpn J. Appl. Phys. **12**, *10*, 1621 (1973). DOI: 10.1143/JJAP.12.1621
[51] T.D. Cuong, A.D. Phan. Vacuum **179**, 109444 (2020). DOI: 10.1016/j.vacuum.2020.109444
[52] M.N. Magomedov. Tech. Phys. Lett. **27**, *9*, 773 (2001). DOI: 10.1134/1.1407355
[53] A.F. Andreev, I.M. Lifshitz. Sov. J. Exp. Theor. Phys. **29**, *6*, 1107 (1969). DOI: 10.1070/PU1971v013n05ABEH004235
[54] A.F. Andreev. Prog. Low Temperature Phys. **8**, 67 (1982). DOI: 10.1016/s0079-6417(08)60005-0
[55] M.N. Magomedov. Tech. Phys. Lett. **34**, *5*, 414 (2008). DOI: 10.1134/S1063785008050167
[56] P. Varotsos, K. Alexopoulos. J. Phys. C **12**, *19*, L761 (1979). DOI: 10.1088/0022-3719/12/19/004
[57] S.M. Heald, D.R. Baer, R.O. Simmons. Phys. Rev. B **30**, *5*, 2531 (1984). DOI: 10.1103/PhysRevB.30.2531
[58] P.R. Granfors, B.A. Fraass, R.O. Simmons. J. Low Temperature Phys. **67**, *5/6*, 353 (1987). DOI: 10.1007/BF00710349
[59] I. Iwasa, H. Suzuki. J. Low Temperature Phys. **62**, *1/2*, 1 (1986). DOI: 10.1007/BF00681316
[60] I. Iwasa. J. Phys. Soc. Jpn **56**, *5*, 1635 (1987). DOI: 10.1143/JPSJ.56.1635
[61] M.E.R. Bernier, J.H. Hetherington. Phys. Rev. B **39**, *16*, 11285 (1989). DOI: 10.1103/PhysRevB.39.11285
[62] M.I. Mendelev, B.S. Bokstein. Phil. Mag. **90**, *5*, 637 (2010). DOI: 10.1080/14786430903219020